NANO LETTERS

Letter

pubs.acs.org/NanoLett

Inorganic Micelles as Efficient and Recyclable Micellar Catalysts

Qiao Zhang,[†,‡] Xing-Zhong Shu,[†,§] J. Matthew Lucas,[∥] F. Dean Toste,*[,†,§] Gabor A. Somorjai,*[,†,‡] and A. Paul Alivisatos*[,†,‡]

[†]Department of Chemistry, University of California, Berkeley, Berkeley, California 94720, United States

[‡]Materials Sciences Division and [§]Chemical Sciences Division, Lawrence Berkeley National Laboratory, Berkeley, California 94720, United States

[∥]Department of Mechanical Engineering, University of California, Berkeley, California 94720, United States

Supporting Information

ABSTRACT: An "inorganic micelle" structure that has a hydrophilic cavity and hydrophobic surface has been synthesized. The inorganic micelles possess large surface area and controllable hydrophobic/hydrophilic interface. It shows high catalytic efficiency and great recyclability in the bromination of alcohols. This work suggests that inorganic micelles may be suitable for selective organic syntheses as well as industrial applications and demonstrates the value of translating nanostructure design from organic to inorganic.

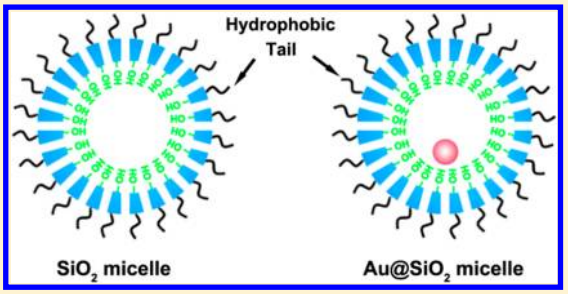

KEYWORDS: *Inorganic micelle, silica, catalysis, hollow structure*

Motivated by the exciting possibility of obtaining catalytic effects close to those observed with natural biocatalysts, micellar catalysis that utilizes the hydrophilic/hydrophobic interface of organic micelles has attracted long-standing and continuing attention since the 1960s.[1−5] However, the practical application of micellar catalysis has been limited by some of the problematic features of organic micelles.[6] For example, micelles are extremely sensitive to the reaction conditions, such as temperature, pH, and water/oil ratio, resulting in a very narrow stability window, substantially limiting the range of reactions that can be investigated. It is thus appealing to translate the organic structure into an inorganic structure that also has the hydrophilic/hydrophobic interface and large surface area.[7−9] As rigid structures, such solid inorganic micelles should possess some advantageous features over their organic counterparts, such as exceptional mechanical and thermal stability, easy separation, and high recyclability. The difficulty in making such an inorganic micelle is the creation of a permeable inorganic shell with selective modification of the inner- and outer-surfaces. In situations where the reaction between two reagents is enhanced at the hydrophilic−hydrophobic interface, an additional synthetic challenge arises from the need to keep the surface properties of the permeable shell channels compatible with that of the inner cavity to maximize hydrophilic−hydrophobic contact area and to facilitate the transportation of reagents. Recently, the creation of the hydrophilic−hydrophobic interface has attracted some attention. For example, Yang and co-workers reported the synthesis of a solid mesoporous silica spheres consisting of a hydrophobic core and a hydrophilic shell through a sol−gel approach.[10] However, no catalytic application of such structure has been reported yet.

Here we present the preparation and catalytic application of an inorganic micelle structure. The structure is prepared by utilizing the knowledge from the well-developed silica-based core−shell nanostructures.[11,12] To achieve selective surface modification, CTAB micelles were first explored as a "pore blocking" agent during the surface modification process and then removed to "open" the mesoporous channels. In this way, the surface properties of the mesoporous channels could be kept the same as that of the inner surface. The accessibility of the inner nanocavity was confirmed by monitoring the reduction of aqueous 4-nitrophenol using Au@SiO_2 micelles as the catalysts. We further demonstrated that the hydrophobicity of inorganic micelles could be conveniently adjusted. As a result, the mass transfer of hydrophilic species was easily tuned, which is beneficial for catalytic selectivity and not possible in organic micelles. We also examined the application of these inorganic micelles to model catalytic reactions, the brominations of primary- and secondary-alcohols with HBr solution, and found that the inorganic micelles showed superior catalytic properties to their organic counterparts.

Two types of inorganic micelles, including pure SiO_2 micelles and core−shell Au@SiO_2 micelles, were successfully prepared. The incorporation of metal nanoparticles within the major cavity of the inorganic micelle not only assists with the characterization of the micelle structures but also holds promising potential for fabricating attractive tandem catalysts that utilize both metal nanocatalysts and the micelle itself.[13,14] As shown in Figure 1a, the preparation process first required

Received: December 7, 2013
Published: December 8, 2013

dx.doi.org/10.1021/nl4045372 | *Nano Lett.* 2014, 14, 379−383

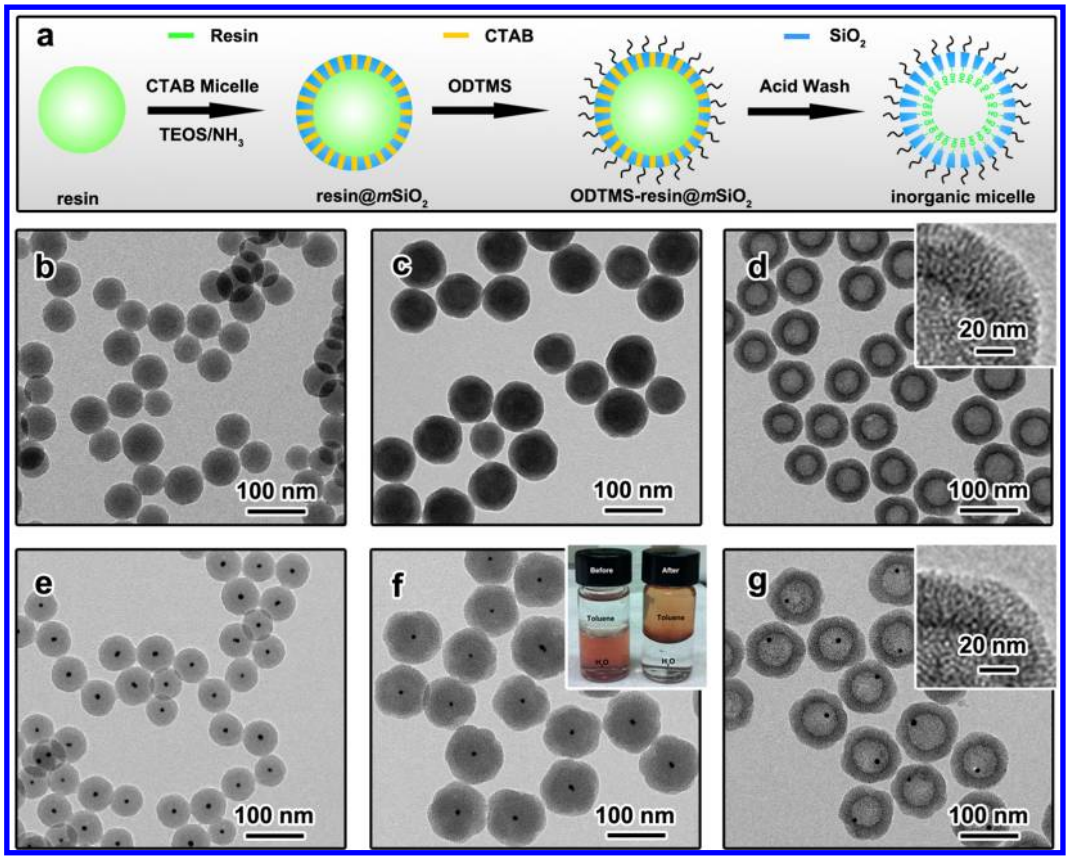

Figure 1. Synthetic protocol and TEM characterization. (a) Schematic illustration of the synthesis of inorganic micelles. (b–d) and (e–g) TEM images shown the stepwise preparation process of silica micelles and Au@SiO_2 micelles, respectively: (b) resin nanoparticles; (c) resin@SiO_2 particles; (d) hollow SiO_2 micelles; (e) Au@resin nanoparticles; (f) Au@resin@SiO_2 particles; and (g) Au@ SiO_2 micelles. The inset digital image in (f) shows that hydrophilic Au@resin@SiO_2 nanoparticles could be successfully transferred from water to toluene after hydrophobic surface modification.

the generation of spherical resin nanoparticles employing a previously reported colloidal synthesis.[15,16] Figure 1b shows a TEM image of a typical resin sphere sample with average diameter of 40 nm. The Au@resin nanoparticles were prepared through an in situ polymerization process in which Au^{3+} ions were first reduced to form Au nanoparticles, followed by the polymerization of resin spheres around the Au nanoparticles.[17] Figure 1e shows a TEM image of a sample of Au@ resin nanoparticles with average diameter of 50 nm.

The mesoporous silica shell was subsequently obtained through a surfactant-assisted approach, using a cationic surfactant, CTAB (cetyltrimethylammonium bromide), as the structure-directing agent.[18,19] CTAB molecules can form cylindrical micelles and attach to the surface of resin spheres due to electrostatic attractive forces. Silica coating around the CTAB scaffold was achieved by the hydrolysis of TEOS (tetraethyl orthosilicate) in the presence of NH_4OH. The successful coating of the mesoporous silica shell was confirmed by TEM characterization, as shown in Figure 1c,f. The particle size was increased from around 40 nm to around 100 nm, suggesting a shell thickness of about 30 nm. Additionally, the mesopores within the shell were radially ordered.[19]

The outer surfaces of the silica shells could be modified to be hydrophobic by taking advantage of well-developed silane chemistry.[20,21] Typically, the resin@SiO_2 particles were dried in air and then transferred to a solution of 1,2-dichlorobenzene containing *n*-octadecyltrimethoxy-silane (ODTMS). The surface silanols were attacked by the hydrolyzable alkoxy groups of the organosilanes through an alcoholysis reaction, resulting in the formation of a monolayer of hydrophobic alkyl chains on the silica surface through covalent −Si−O−Si− bonds, which has been confirmed by FTIR (Supporting Information Figure S1). The as-obtained particles were well dispersed in most nonpolar solvents (toluene, chloroform, and hexane) and some less-polar solvents (acetone). As shown in the inset in Figure 1f, the core−shell particles were well dispersed in toluene after treatment, further confirming the successful surface modification.

Because of the formation of the CTAB−silica complex during the coating process,[19,22] it is believed that the existence of the CTAB micelle could "block" the mesoporous channel. As a result, the inner cavity surface and the channel surface were not modified and remained hydrophilic. This was verified by the successful extraction of CTAB and removal of the resin templates using hydrophilic species. For the extraction process, the as-prepared products were refluxed in a mixture of acetone and HCl for 24 h.[23] The extraction process was repeated twice to fully remove CTAB and open the mesopores. After removing the CTAB micelles, the product was well dispersed in ethanol and partially dispersed in water, suggesting hydrophilic mesopores had been opened. Figure 1d,g shows the typical morphology of pure silica micelles and Au@SiO_2 micelles, respectively. By tuning the size of the original resin or Au@ resin nanoparticles, the size of the final micelles was controlled in the range of about 50 to 170 nm, as shown in Supporting Information Figures S2 and S3.

dx.doi.org/10.1021/nl4045372 | *Nano Lett.* 2014, 14, 379−383

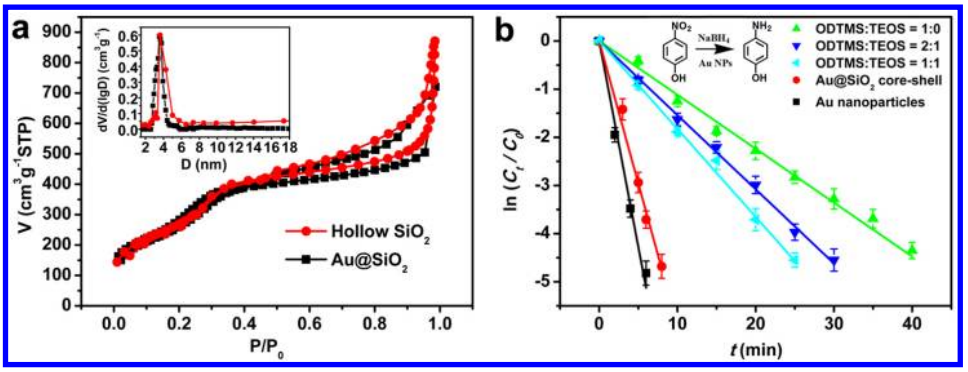

Figure 2. BET characterization and controllable mass transfer test. (a) Nitrogen adsorption/desorption isotherms for hollow silica (red) and Au@SiO_2 (black), respectively. The inset shows the corresponding pore size distributions; (b) Plot of $\ln(C_t/C_0)$ as a function of reaction time t for the reduction of 4-NP by $NaBH_4$ in the presence of different catalysts. (From left to right) Au nanoparticles (black); hydrophilic Au@SiO_2 core−shell structures obtained by removing CTAB and resin template (red); and inorganic micelles obtained with different ratios of ODTMS/TEOS: 1/1 (cyan); 2/1 (blue); and 1/0 (green). The amount of Au@SiO_2 micelles used is 2.5 times as many of pure Au and hydrophilic Au@SiO_2 to get results within a reasonable time period.

The surface area and porosity of the inorganic micelles were further investigated by nitrogen adsorption−desorption isotherms. As shown in Figure 2a, there is a single and sharp adsorption step at intermediate relative partial pressure values around 0.3 for both hollow silica and Au@SiO_2, which is in good agreement with the typical type IV curves of surfactant-assisted mesoporous silica.[24] For the hollow silica micelles, the Brunauer− Emmett−Teller (BET) surface area and single-point total pore volume are 1066 m^2 g^{-1} and 1.1 cm^3 g^{-1}, respectively, suggesting a highly porous structure. The average Barret−Joyner−Halenda (BJH) pore diameter calculated from the desorption branch of the isotherm was measured to be 4.7 nm (see inset in Figure 2a). The sharp peak indicates the uniform pore size distribution. For the Au@SiO_2 core−shell structure, the BET surface area is 979 m^2 g^{-1}. Although the surface area is slightly decreased, the total pore volume and pore diameter of the Au@SiO_2 yolk−shell structure is consistent with the pure hollow silica case with the values of 1.1 cm^3 g^{-1} and 4.5 nm, respectively, suggesting good reproducibility for this synthetic protocol.

The permeability of the inorganic micelle is of great importance since catalytic reactions of interest can occur only at the hydrophilic/hydrophobic interface. The successful preparation of Au@SiO_2 micelles enables us to quantitatively analyze their surface properties. An aqueous phase reduction of 4-nitrophenol (4-NP) by $NaBH_4$ was used as a model reaction to characterize the inorganic micelle structure.[25,26] This reduction can be considered as pseudo-first-order reaction with regard to 4-NP, because the concentration of $NaBH_4$ greatly exceeded that of 4-NP. In the absence of Au nanoparticles, the reduction process did not proceed even with a large excess of $NaBH_4$. Figure 2b shows the linear relationship between $\ln(C_t/C_o)$ and reaction time t for reductions under various conditions and by different catalysts. It is clear that all these plots obey first-order reaction kinetics very well. The rate constant k was calculated from the rate equation $\ln(C_0/C_t) = kt$, while the turnover frequency was defined as the number of moles of reduced reactant per mole surface Au atoms per hour when the conversion has reached 90%. The performance of different catalysts is summarized and plotted in Supporting Information Table S1 and Figure 2b, respectively. Au nanoparticles are excellent catalysts for this reduction process, as confirmed by the rapid reduction process using Au nanoparticles (reduction completed within several minutes). However, upon addition of freshly prepared Au sol, a dark precipitate was formed, indicating the occurrence of severe agglomeration. When hydrophilic Au@SiO_2 core−shell structures were used as the catalyst, no agglomeration was observed, demonstrating enhanced stability. The reaction constant (k = 0.606 min^{-1}) and the TOF (1527 h^{-1}) for the Au@SiO_2 core−shell structures were slightly lower than those of pure Au nanoparticles (k = 0.800 min^{-1}, TOF = 2003 h^{-1}), mainly due to the diffusion through mesoporous shell. Although the diffusion of hydrophilic species through the inorganic micelle structure was much slower, as shown by the reaction constant and TOF (k = 0.108 min^{-1}, TOF = 108 h^{-1}), it is clear that the inner cavity of the inorganic micelle was accessible by hydrophilic reactants. The accessibility of the inner cavity was further demonstrated by a seeded-growth experiment in which Au@Ag nanoparticles were obtained using the encapsulated Au nanoparticles as the seeds for the deposition of silver reduced by ascorbic acid (Supporting Information Figure S4).

We further demonstrate that the hydrophobicity of the inorganic micelle structure could be engineered. As a result, the diffusion rate of molecules through the shells could be conveniently adjusted, which cannot be easily achieved in organic micelles. The hydrophobicity control was achieved through the coalcoholysis of ODTMS and TEOS. After hydrolysis of TEOS, more −OH groups were introduced onto the surface and therefore the density of long alkane chains from earlier ODTMS treatment was lowered.[27] As shown in Supporting Information Table S1 and Figure 2b, increasing the concentration of TEOS raised both the rate constant (k) and TOF (k = 0.152 min^{-1}, TOF = 152 h^{-1} for TEOS/ODTMS = 1:2; and k = 0.181 min^{-1}, TOF = 181 h^{-1} for TEOS/ODTMS = 1:1.), suggesting higher catalytic efficiencies. This observation is consistent with enhanced diffusion of hydrophilic reactants through the mesoporous shell.

The inorganic micelles demonstrated here were also able to act as highly efficient and recyclable catalysts for some organic reactions. The bromination of alcohols with HBr solution has been selected as a model system, as alkyl halides, particularly bromides, are very useful reagents in organic chemistry, chemical biology, and pharmaceuticals.[28−32] Most traditional protocols require highly toxic reagents and high temperature.[33,34] With the help of inorganic micelles, the bromination of both primary- and secondary-alcohols was achieved under mild conditions. Dichloromethane (CH_2Cl_2) was used as the

dx.doi.org/10.1021/nl4045372 | Nano Lett. 2014, 14, 379−383

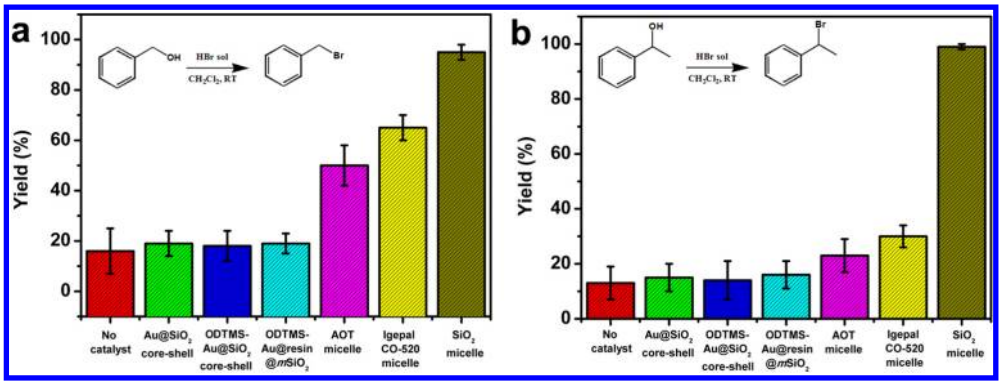

Figure 3. Catalytic study. The yields of (a) benzyl bromide and (b) α-methylbenzyl bromide in the bromination of alcohols using HBr solution with the assistance of different catalysts.

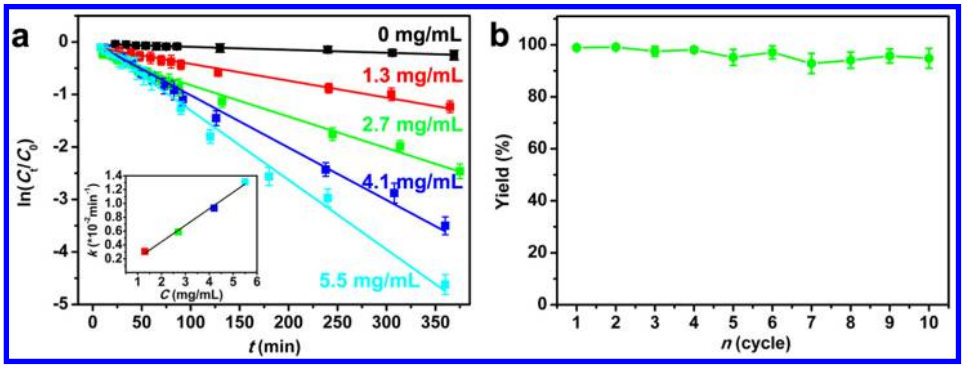

Figure 4. Kinetic and reusability study. (a) Plot of $\ln(C_t/C_0)$ as a function of the reaction time for pseudo-first-order bromination of benzyl alcohol without micelles (black) or with different amounts of micelles: 1.3 mg/mL (red), 2.7 mg/mL (green), 4.1 mg/mL (blue) and 5.5 mg/mL (cyan). The inset is the plot of rate constant k as a function of the concentration C of micelles. (b) Conversion of benzyl alcohol in 10 successive cycles of bromination with 5.5 mg/mL of silica micelles.

solvent (see Supporting Information Table S2 for other solvents). As shown in Figure 3a, in the absence of any catalyst the reaction rate for bromination of benzyl alcohol was very low, as evidenced by the ~16% yield of benzyl bromide after 6 h. When the inorganic micelles, either pure silica or Au@SiO_2, were used as catalysts, a dramatic increase of the yield of benzyl bromide was detected. As shown in Figure 3a, the yield increased to more than 95% for the inorganic micelle catalyzed process. To investigate the influence of the inorganic micelle structures, a series of control experiments were conducted. As displayed in Figure 3a and Supporting Information Figure S5, the use of SiO_2 nanoparticles, Au nanoparticles, Au@resin nanoparticles, entirely hydrophilic Au@SiO_2 core−shell structures, ODTMS-modified entirely hydrophobic Au@SiO_2 core−shell structures, and ODTMS-modified entirely hydrophobic Au@resin@meso-SiO_2 as catalysts did not show a significant improvement over the uncatalyzed reaction. These results are consistent with the requirement that a true micellar structure is required for catalysis. To compare with organic micelles, two types of reverse micelles composed of an anionic surfactant, AOT (dioctyl sodium sulfosuccinate), and a nonionic surfactant, Igepal CO-520 (polyoxyethylene (5)), were used as catalysts. In both systems, HBr solution was encapsulated inside the micelles first, followed by the mixing with benzyl alcohol. The yields for using AOT micelle and Igepal-520 micelle were approximately 50% and 65%, respectively.

The inorganic micelles not only catalyze the bromination of primary alcohols but are also applicable to secondary alcohols, suggesting a general approach for the bromination of alcohols. A secondary alcohol, α-methylbenzene alcohol, was used as the model molecule for this bromination process. In the presence of inorganic micelles, the bromination process completed with full conversion (>99%) within 15 min, which is much faster than the case of primary alcohols. The catalytic effect of inorganic micelles was verified by the control experiments (Figure 3b). Although the organic micelles based on AOT and Igepal CO-520, showed some catalytic effect, it was not very significant with a yield of 23 and 30%, respectively. The low yield might be attributed to the relatively slow diffusion of reagents through the micelle structure, suggesting the mass transport advantage of inorganic micelles.

To gain further insight into the catalytic effect of inorganic micelles, the bromination of benzyl alcohol was studied in more depth. As shown in Figure 4a and Supporting Information Table S3, in the absence of inorganic micelles, the bromination reaction is a pseudo-first-order reaction with respect to benzyl alcohol as the plots fit first-order reaction kinetics. The rate constant k calculated from the rate equation $\ln(C_0/C_t) = kt$ is 5.4×10^{-4} min^{-1}. With the assistance of silica micelles, the bromination process was significantly accelerated while remaining pseudo-first-order. When the concentration of silica micelles in the system was 2.7 mg/mL, the rate constant increased to 5.9×10^{-3} min^{-1}, an order of magnitude enhancement. The rate constant was further increased to 1.3×10^{-2} min^{-1} when the concentration of silica micelle was increased to 5.5 mg/mL, which is a factor of 24 greater compared to the catalyst-free solution. The inset in Figure 4a

dx.doi.org/10.1021/nl4045372 | Nano Lett. 2014, 14, 379−383

plotted the rate constant k as a function of the concentration C of micelles used, which fits a linear relationship very well, suggesting that the reaction occurred at the hydrophilic/hydrophobic interface. The reusability of inorganic micelles was also investigated. As displayed in Figure 4b, no notable deactivation of the catalyst was observed with up to ten cycles, indicating excellent recyclability. Compared with organic micelles that cannot be recovered, the inorganic micelles are more promising in practical applications.

In summary, a unique inorganic micelle with large surface area and hydrophobic/hydrophilic interface has been developed. By constructing a metal-in-oxide Au@SiO_2 micelle, the surface property of micelles has been carefully characterized. The as-obtained inorganic micelles showed excellent catalytic activity in catalyzing bromination of alcohols. As a result of their rigid structure, inorganic micelles are superior to organic micelles with respect to their easy separation and high recyclability. This work suggests that inorganic micelles may be suitable for selective organic syntheses and potentially even for industrial applications and demonstrates the value of translating nanostructure design from organic to inorganic.

■ ASSOCIATED CONTENT

Supporting Information

Detailed experimental procedures and additional data including TEM images, FTIR, and catalysis data. This material is available free of charge via the Internet at http://pubs.acs.org.

■ AUTHOR INFORMATION

Corresponding Authors

*(F.D.T.) E-mail: fdtoste@berkeley.edu;
*(G.A.S.) E-mail: somorjai@berkeley.edu.
*(A.P.A.) E-mail: alivis@berkeley.edu.

Author Contributions

The manuscript was written through contributions of all authors. All authors have given approval to the final version of the manuscript.

Notes

The authors declare no competing financial interest.

■ ACKNOWLEDGMENTS

We thank the financial support from the Dow Chemical Company through funding for the Core−Shell Catalysis Project, contract #20120984 to University of California, Berkeley. J.M.L. is supported as part of the Light-Material Interactions in Energy Conversion, an Energy Frontier Research Center funded by the U.S. Department of Energy, Office of Science, Office of Basic Energy Sciences, under Contract DE-SC0001293. We are grateful to Dr. Y. Surendranath and Dr. E. Gross for helpful discussions.

■ REFERENCES

(1) Fendler, J. H.; Fendler, E. J. *Catalysis in Micellar and Macromolecular Systems*; Academic Press: New York, 1975.
(2) Ruasse, M. F.; Blagoeva, I. B.; Ciri, R.; GarciaRio, L.; Leis, J. R.; Marques, A.; Mejuto, J.; Monnier, E. *Pure Appl. Chem.* **1997**, *69*, 1923.
(3) Pileni, M. P. *Structure and Reactivity in Reverse Micelles*; Elsevier: Amsterdam, 1989.
(4) Schwuger, M. J.; Stickdorn, K.; Schomacker, R. *Chem. Rev.* **1995**, *95*, 849.
(5) Breslow, R. *Acc. Chem. Res.* **1995**, *28*, 146.
(6) Dwars, T.; Paetzold, E.; Oehme, G. *Angew. Chem., Int. Ed.* **2005**, *44*, 7174.
(7) Yah, W. O.; Takahara, A.; Lvov, Y. M. *J. Am. Chem. Soc.* **2012**, *134*, 1853.
(8) Abbaspourrad, A.; Carroll, N. J.; Kim, S. H.; Weitz, D. A. *Adv. Mater.* **2013**, *25*, 3215.
(9) Liang, F. X.; Liu, J. G.; Zhang, C. L.; Qu, X. Z.; Li, J. L.; Yang, Z. Z. *Chem. Commun.* **2011**, *47*, 1231.
(10) Li, S. R.; Jiao, X.; Yang, H. Q. *Langmuir* **2013**, *29*, 1228.
(11) Guerrero-Martinez, A.; Perez-Juste, J.; Liz-Marzan, L. M. *Adv. Mater.* **2010**, *22*, 1182.
(12) Li, X. B.; Yang, Y.; Yang, Q. H. *J. Mater. Chem. A* **2013**, *1*, 1525.
(13) Bao, J.; He, J.; Zhang, Y.; Yoneyama, Y.; Tsubaki, N. *Angew. Chem., Int. Ed.* **2008**, *47*, 353.
(14) Yamada, Y.; Tsung, C. K.; Huang, W.; Huo, Z. Y.; Habas, S. E.; Soejima, T.; Aliaga, C. E.; Somorjai, G. A.; Yang, P. D. *Nat. Chem.* **2011**, *3*, 372.
(15) Liu, J.; Qiao, S. Z.; Liu, H.; Chen, J.; Orpe, A.; Zhao, D. Y.; Lu, G. Q. *Angew. Chem., Int. Ed.* **2011**, *50*, 5947.
(16) Fang, X. L.; Liu, S. J.; Zang, J.; Xu, C. F.; Zheng, M. S.; Dong, Q. F.; Sun, D. H.; Zheng, N. F. *Nanoscale* **2013**, *5*, 6908.
(17) Guo, S. R.; Gong, J. Y.; Jiang, P.; Wu, M.; Lu, Y.; Yu, S. H. *Adv. Funct. Mater.* **2008**, *18*, 872.
(18) Gorelikov, I.; Matsuura, N. *Nano Lett.* **2008**, *8*, 369.
(19) Zhang, M.; Wu, Y. P.; Feng, X. Z.; He, X. W.; Chen, L. X.; Zhang, Y. K. *J. Mater. Chem.* **2010**, *20*, 5835.
(20) Wang, W.; Gu, B. H.; Liang, L. Y.; Hamilton, W. *J. Phys. Chem. B* **2003**, *107*, 3400.
(21) Garcia, N.; Benito, E.; Guzman, J.; Tiemblo, P. *J. Am. Chem. Soc.* **2007**, *129*, 5052.
(22) Grosso, D.; Babonneau, F.; Albouy, P. A.; Amenitsch, H.; Balkenende, A. R.; Brunet-Bruneau, A.; Rivory. *J. Chem Mater* **2002**, *14*, 931.
(23) Fang, X. L.; Chen, C.; Liu, Z. H.; Liu, P. X.; Zheng, N. F. *Nanoscale* **2011**, *3*, 1632.
(24) Sing, K. S. W.; Everett, D. H.; Haul, R. A. W.; Moscou, L.; Pierotti, R. A.; Rouquerol, J.; Siemieniewska, T. *Pure. Appl. Chem.* **1985**, *57*, 603.
(25) Lu, Y.; Mei, Y.; Drechsler, M.; Ballauff, M. *Angew. Chem., Int. Ed.* **2006**, *45*, 813.
(26) Zhang, Q.; Zhang, T. R.; Ge, J. P.; Yin, Y. D. *Nano Lett.* **2008**, *8*, 2867.
(27) Nakamura, H.; Matsui, Y. *J. Am. Chem. Soc.* **1995**, *117*, 2651.
(28) Lednicer, D. *Strategies for Organic Drug Synthesis and Design*, 2nd ed.; John Wiley & Sons: New York, 2009.
(29) Zarghi, A.; Faizi, M.; Shafaghi, B.; Ahadian, A.; Khojastehpoor, H. R.; Zanganeh, V.; Tabatabai, S. A.; Shafiee, A. *Bioorg. Med. Chem. Lett.* **2005**, *15*, 3126.
(30) Sharghi, H.; Khalifeh, R.; Doroodmand, M. M. *Adv. Synth. Catal.* **2009**, *351*, 207.
(31) Mohanazadeh, F.; Zolfigol, M. A.; Sedrpoushan, A.; Veisi, H. *Lett. Org. Chem.* **2012**, *9*, 598.
(32) Godefroi, E. F.; Van Cutsem, J.; Van der Eycken, C. A. M.; Janssen, P. A. J. *J. Med. Chem.* **1969**, *12*, 784.
(33) Cainelli, G.; Contento, M.; Manescalchi, F.; Plessi, L. *Synthesis-Stuttgart* **1983**, 306.
(34) Thiel, V.; Brinkhoff, T.; Dickschat, J. S.; Wickel, S.; Grunenberg, J.; Wagner-Dobler, I.; Simon, M.; Schulz, S. *Org. Biomol. Chem.* **2010**, *8*, 234.